ELSEVIER

International Journal of Mass Spectrometry 182/183 (1999) 369–380

International Journal of Mass Spectrometry

Adducts and dimers of SF_n^+ (n = 1–5) with benzene, acetonitrile, and pyridine. Gas-phase generation and ab initio structures and thermochemistry

Regina Sparrapan, Maria Anita Mendes, Marcos N. Eberlin*

Institute of Chemistry, State University of Campinas–UNICAMP, CP 6154, 13083-970, Campinas, SP Brazil

Received 20 July 1998; accepted 16 September 1998

Abstract

Pentaquadrupole (QqQqQ) mass spectrometry is used to explore the abilities of gaseous SF_n^+ (n = 1–5) ions to form adducts and dimers with three π-electron rich molecules—benzene, acetonitrile, and pyridine, whereas ab initio calculations estimate most feasible structures, bond dissociation energies (BDEs), and reaction enthalpies of the observed products. With benzene, SF^+ reacts by net H-by-$SF^{+\cdot}$ replacement. As suggested by the calculations, this novel benzene reaction forms ionized benzenesulfenyl fluoride, C_6H_5–$SF^{+\cdot}$, via a Wheland-type intermediate that spontaneously loses a H atom. SF_3^+ forms a rare, loosely bonded π complex with benzene, $[Bz \cdots SF_3]^+$, which is stable toward both H and HF loss. No dimer, $Bz_2SF_3^+$, is formed. According to calculations, an unsymmetrically bonded, π-coordinated $Bz_2SF_3^+$ dimer exists, i.e. $(Bz–SF_3 \cdots Bz)^+$, but its formation from $[Bz \cdots SF_3]^+$ is endothermic; hence, thermodynamically unfavorable. With acetonitrile, $SF_2^{+\cdot}$, SF_3^+, and SF_5^+ form both adducts and dimers. CH_3–C^-═N–SF_2^+ (a new distonic ion) and CH_3CN–SF_5^+ are covalently bonded, but $CH_3CN \cdots SF_3^+$ is loosely bonded. The binding natures of the acetonitrile adducts are reflected in the dimers; $[CH_3CN–SF_2 \cdots NCCH_3]^{+\cdot}$ and $[CH_3CN–SF_5 \cdots NCCH_3]^+$ are unsymmetrically bonded, whereas $[CH_3CN \cdots SF_3 \cdots NCCH_3]^+$ is symmetrically and loosely bonded. Such dimers as $[CH_3CN \cdots SF_3 \cdots NCCH_3]^+$ are ideal for measurements of ion affinity via the Cooks' kinetic method. With pyridine, only SF_3^+ forms adduct and dimer. Py–SF_3^+ is covalently bonded through nitrogen; $[Py \cdots SF_3 \cdots Py]^+$ is loosely but unsymmetrically bonded. The unsymmetric 2.28 and 2.44 Å long N–S bonds in $[Py \cdots SF_3 \cdots Py]^+$, which are expected to rapidly interconvert, result likely from steric hindrance that forces orthogonal alignment of the two pyridine rings. Most observed adducts and dimers display relatively high BDEs, i.e. they are formed in thermodynamically favorable reactions. The extents of dissociation of the adducts and dimers observed in MS^3 experiments reflect the structures and BDEs predicted by the calculations. (Int J Mass Spectrom 182/183 (1999) 369–380) © 1999 Elsevier Science B.V.

Keywords: SF_6; SF_n^+: SF_5^+, $SF_4^{+\cdot}$, SF_3^+, $SF_2^{+\cdot}$, SF^+; Ion/molecule reactions; Pentaquadrupole mass spectrometry

1. Introduction

The fundamental properties and practical applications of sulfur hexafluoride (SF_6), a fascinating hypervalent molecule, have been investigated extensively [1–7]. SF_6 has shown to be of widespread practical use. It is used, for instance, as a highly efficient insulator [1], as the source of F atoms in lasers and in plasma etching processes [2], as an electron capture reagent in ion sources [3], and in isotope separation processes by laser irradiation [4] and multiphoton processes [5]. SF_6 also serves as a

* Corresponding author.

Dedicated to the memory of Professor Ben Freiser, in particular for his incisive contributions to gas-phase ion/molecule chemistry.

PII S1387-3806(98)14235-5

model for UF_6 [6], and of unusual hypervalent species [7].

The protective layer of F atoms in neutral SF_6 drastically limits its chemical reactivity by obstructing access to the reactive sulfur center [8]. Yet, ions having higher ionization energies react with SF_6 but only "superficially," SF_5^+ is formed either by charge exchange or F^- abstraction [9]. Jiao and Freiser [10] showed, however, that early transition metal cations with at least one empty *d* orbital, Sc^+ for instance, are able to coordinate to sulfur breaking down the S–F bonds via $[Sc^{\cdot\cdot}SF_6^+]$ complexes; SF_n^+ ions (n = 2–5) are the observed products.

Ionized sulfur hexafluoride ($SF_6^{+\cdot}$), which is more energetic than its primary dissociation products SF_5^+ and $F^{\cdot}$ [11], dissociates promptly on electron ionization to sulfur fluoride cations, SF_n^+ (n = 1–5). SF_n^+ are also formed as by-products when using SF_6 as a gaseous dielectric or in plasma etching gases [12]. An interesting application of SF_n^+ is their implanting into GaAs field-electron transistors to improve performance [13]. Despite easy access, and the potential of gas-phase investigations in accessing the intrinsic properties of SF_n^+, studies on the chemistry of gaseous SF_n^+ have been sporadic and scattered [14–18]. The understanding and control of the chemical and electrical processes in which SF_n^+ participate would certainly benefit from systematic studies on their gas-phase reactivities.

Contrary to SF_6, in SF_n^+ the extraordinary coordination ability and the higher electron deficiency of the central sulfur atom, and the weakening of the protective F layer enhance reactivity favoring, for instance, adduct and dimer formation with π-electron rich species. Several of such adducts have been reported in the gas phase. Weakly bonded $[SF_m(SF_6)_n]^+$ cluster ions (m = 0–5; n = 1–3) have been formed in high pressure mass spectrometric (HPMS) conditions [14]. SF_5^+ and SF_3^+ form adducts with amines [15] that rapidly lose HF. SF_5^+ forms an adduct with H_2S that partially dissociates to SF_4SH^+ [16]. The water complex, H_2O/SF_5^+, which eventually dissociates to SF_3O^+, has also been reported [3,17]. Under HPMS conditions [3], SF_5^+ forms adducts with benzene, toluene, acetone, acetic acid and nitriles; the benzene/SF_5^+ and toluene/SF_5^+ adducts lose HF at longer reaction times. SF_3^+ forms stable adducts and dimers with many pyridines [18]; hence, by forming and dissociating mixed $[Py^1 \cdots SF_3^+ \cdots Py^2]$ dimers, SF_3^+ pyridine affinities were measured via the Cooks' kinetic method [19]. A recent gas-phase systematic study [20] showed that SF_n^+ (n = 0–5) form no stable adducts or dimers with the oxygenated molecules H_2O, CO, CO_2, O_2, and N_2O. Instead, SF^+ abstracts an oxygen atom from both O_2 and CO to form FSO^+; similar O abstraction of $S^{+\cdot}$ from CO_2 and O_2 yields $SO^{+\cdot}$. SF^+ also reacts with CO by net $S^{+\cdot}$ transfer to form $COS^{+\cdot}$ [20].

We report here a multiple stage pentaquadrupole (QqQqQ) mass spectrometry [21] investigation on the proclivity of gaseous SF_n^+ (n = 1–5) ions to form stable adducts and dimers with three π-electron rich molecules—benzene, acetonitrile, and pyridine. Stable adducts and dimers were often, but not generally formed. Theory, i.e. ab initio calculations at the MP2/6–31G(d,p)//6-31G(d,p) + zero point energy (ZPE) level, were performed to help rationalize the contrasting SF_n^+ coordination abilities by providing reaction enthalpies, bond dissociation energies (BDEs), and most likely structures for adducts and dimers.

2. Methods

The MS^2 and MS^3 experiments were performed using an Extrel (Pittsburgh, PA) QqQqQ mass spectrometer [22], in which three mass analyzing (Q1, Q3, Q5) and two "rf-only" reaction quadrupoles (q2, q4) are sequentially arranged. The QqQqQ provides access to all *tandem-in-space* multidimensional MS^2 and MS^3 experiments [23] from which specific chemical information are obtained [21–24].

Ion/molecule reactions were performed by MS^2 experiments; Q1 is used to mass select the reactant ion and the neutral reactant is added to q2. Collisions occur at nearly 1 eV energies, as calculated from the *m/z* 39:41 ratio in neutral ethylene/ionized ethylene reactions [25]. The MS^2 product spectrum is acquired by scanning Q5, while Q3 is operated in the full ion-transmission rf-only mode.

For the triple-stage MS^3 experiments [24], a product ion of interest is mass selected by Q3 and further dissociated by 15 eV collisions with argon in q4, while Q5 is scanned to acquire the spectrum. Overall pressures in the three differentially pumped regions were typically 2×10^{-6} (ion source), 8×10^{-6} (q2), and 8×10^{-5} (q4) Torr, as measured by ion gauges located centrally in each vacuum chamber. Multiple collisions occur in q2, which increase reaction yields and help to promote collisional quenching of both the reactant and product ions [21,23]. Lower reaction yields but similar sets of ionic products are observed at lower pressure, single collision conditions in q2.

Ab initio molecular orbital calculations were carried out by using GAUSSIAN94 [26]. The ions were optimized at the Hartree–Fock (HF) level of theory by employing the polarization 6-31G(*d*,*p*) basis set [27]. Improved energies were obtained by single point calculations at the second-order Møller–Plesset (MP2)/6-31G(*d*,*p*) level [28]. Harmonic vibrational frequencies were calculated at the HF/6-31G(*d*,*p*) level; they are used to characterize the stationary points and to correct energies to the ZPE vibrational level.

3. Results and discussion

3.1. Ion/molecule reactions

Table 1 summarizes the main reactions of SF_n^+ with benzene, acetonitrile, and pyridine. Reactivity changes drastically as the number of fluorines is changed.

3.1.1. Benzene

With benzene, SF_5^+, $SF_4^{+\cdot}$, and $SF_2^{+\cdot}$ react predominantly by charge transfer. Owing to its very low dissociation threshold [20], $SF_4^{+\cdot}$ also loses F to a considerable extent. Charge transfer is still a major reaction for SF^+ and SF_3^+, but these two ions form adducts with benzene.

Figure 1 compares the product ion spectra for reactions of SF^+ and SF_3^+ with benzene (Bz). For SF_3^+, a stable $BzSF_3^+$ adduct of *m/z* 167 is formed [Fig. 1(b)]. But for SF^+, the nascent $BzSF^+$ adduct is apparently unstable losing H to afford the product ion of *m/z* 128 [Fig. 1(a)]. Charge transfer with both ions affords ionized benzene of *m/z* 78. In SF^+ reactions [Fig. 1(a)], protonated benzene of *m/z* 79 is also formed likely via secondary proton transfer from ionized benzene or the *m/z* 128 product, or from both.

Table 1
Summary of the major reactions of SF_n^+ ions: CT[a] = charge transfer, A = adduct formation, D = dimer formation, FL = collision dissociation by F loss.

Ion	Benzene	CH_3CN	Pyridine
SF^+	CT, (A–H)[b]	CT[c]	CT[d]
$SF_2^{+\cdot}$	CT	A, D	CT
SF_3^+	CT, A	A, D	A, D
$SF_4^{+\cdot}$	CT, FL	FL	CT, FL
SF_5^+	CT	A, D	CT

[a] Charge transfer is normally followed by secondary reactions of the ionized neutral with itself forming the protonated neutral and the neutral proton-bonded dimer.
[b] The hot nascent adduct loses promptly a H atom to form *m/z* 128, see Fig. 1(a).
[c] A very minor CH_3CN/SF^+ adduct of *m/z* 92 is also formed.
[d] A very minor $PySF^+$ adduct of *m/z* 130 is also formed.

We consider three structures for the $BzSF^+$ (**a**) and $BzSF_3^+$ (**b**) adducts: the Wheland-type adducts **1**; the 1,4-dicoordinated benzene adducts **2**; and the loosely bonded π-coordinated adducts **3** (Scheme 1). Loss of H from the $BzSF^+$ adduct suggests that ionized benzenesulfenyl fluoride (**4**) is formed as the product

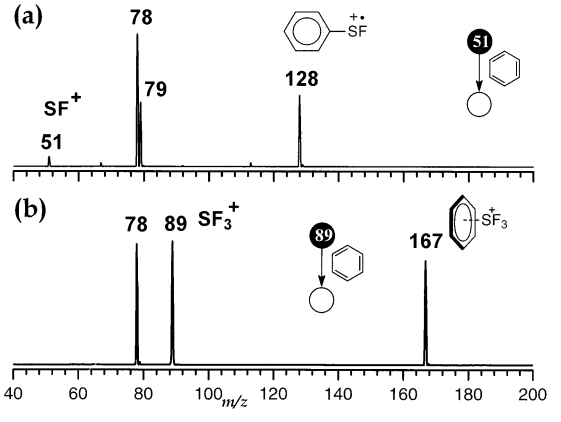

Fig. 1. Double-stage (MS^2) product spectra for reactions with benzene of (a) $^{32}SF^+$ of *m/z* 51 and (b) $^{32}SF_3^+$ of *m/z* 89. The structures shown are those predicted to be the most stable by the ab initio calculations, see the text.

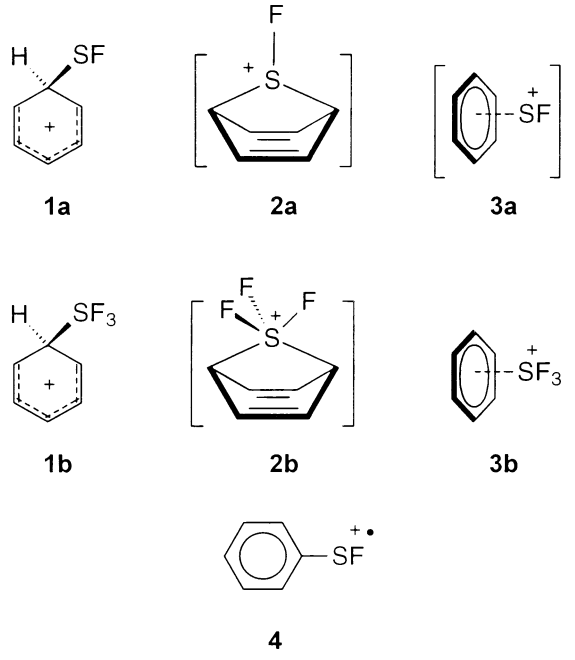

Scheme 1.

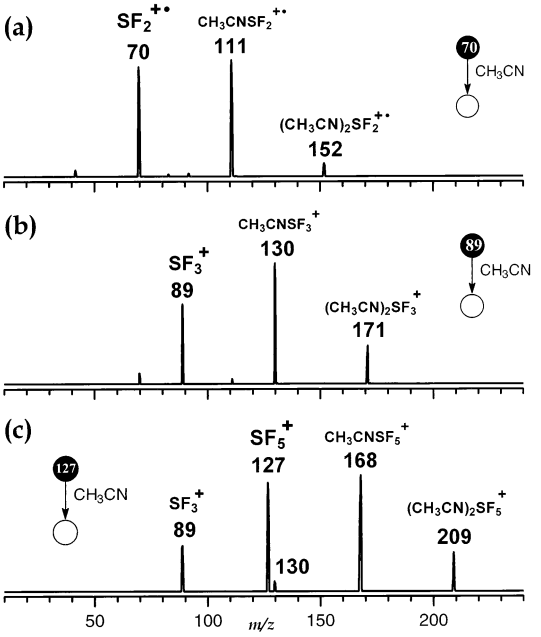

Fig. 2. Double-stage (MS^2) product spectra for reaction with acetonitrile of (a) $^{32}SF_2^{+\cdot}$ of *m/z* 70, (b) $^{32}SF_3^+$ of *m/z* 89, and (c) $^{32}SF_5^+$ of *m/z* 127.

of *m/z* 128. For clarity, structures which are unstable according to the ab initio calculations are represented between brackets.

3.1.2. Acetonitrile

Contrasting SF_n^+ reactivities with CH_3CN (Table 1) are also observed. SF^+ reacts predominantly by charge transfer whereas $SF_4^{+\cdot}$ undergoes no associative reaction; it loses F as the result of collision activation. But $SF_2^{+\cdot}$, SF_3^+, and SF_5^+ react to great extents with CH_3CN to form both adducts and dimers (Fig. 2). That the $CH_3CN/SF_2^{+\cdot}$ (**5**) and CH_3CN/SF_5^+ (**7**) adducts are covalently bonded through nitrogen whereas CH_3CN/SF_3^+ (**6**) is loosely bonded (Scheme 2) is suggested by the calculations. Note the distonic [29] structure **5** (i.e. spatially separated charge and radical sites) expected for a covalently bonded $CH_3CN/SF_2^{+\cdot}$ adduct.

The $(CH_3CN)_2SF_2^{+\cdot}$ (**a**), $(CH_3CN)_2SF_3^+$ (**b**), and $(CH_3CN)_2SF_5^+$ (**c**) dimers could be symmetrically (**8**) or unsymmetrically (**9**) bonded (Scheme 3). If symmetrically (and loosely) bonded, these dimers would be ideal for measurements of SF_n^+ ($n = 2, 3, 5$) nitriles affinities via the Cooks' kinetic method [19]. For $(CH_3CN)_2SF_5^+$, however, the symmetrically and loosely bonded structure **8c** is unlikely. Severe steric hindrance in **8c** owing to heptacoordination to the central sulfur atom should lead to a too weakly bonded dimer (an expectation confirmed by the calculations). Hence, the second acetonitrile molecule should coordinate either through F in an unconventional F-bonded structure **9c** or via simple electrostatic forces to form the unsymmetrically bonded dimer **9c′**.

3.1.3. Pyridine

Both the pyridine pressures and collision energies (near 1 eV) were varied in attempts to form SF_n^+ adducts and dimers with pyridine. However, as observed before [18], only SF_3^+ (Table 1) forms a stable adduct (*m/z* 168) and dimer (*m/z* 247) with pyridine (Fig. 3). Charge transfer followed by secondary $Py^{+\cdot}/Py$ reactions yields the two other products; protonated pyridine of *m/z* 80 and the $[Py \cdots H \cdots Py]^+$ proton bond dimer of *m/z* 159. We

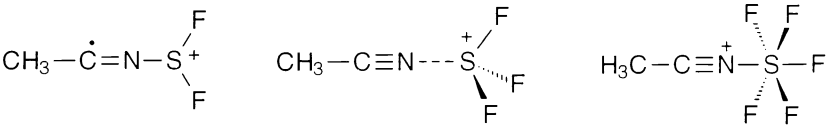

5 **6** **7**

Scheme 2.

considered four structures (Scheme 4) for both the $PySF_3^+$ complex (**10**–**13**) and the $Py_2SF_3^+$ dimer (**14**–**17**).

3.2. Ab initio calculations

3.2.1. Benzene

Ab initio geometry optimization of the three $BzSF^+$ adducts at the HF/6-31G(*d*,*p*) level shows that only **1a** is stable (Fig. 4); **2a** and **3a** collapse to **1a** without any appreciable energy barrier during geometry optimization. Such spontaneous isomerizations of **2a** and **3a** are also observed during geometry optimization at the MP2/6-31G(*d*,*p*) level. These findings suggest that the covalently bonded Wheland-type adduct **1a** is formed (as a dissociating intermediate) in benzene/SF^+ reactions.

Fig. 5(a) shows the MP2/6-31G(*d*,*p*)//6-31G(*d*, *p*) + ZPE potential energy surface diagram for benzene/SF^+ reactions. The enthalpy of formation of **1a** is −52.9 kcal/mol whereas loss of H from **1a** is endothermic by +39.6 kcal/mol; hence, formation of

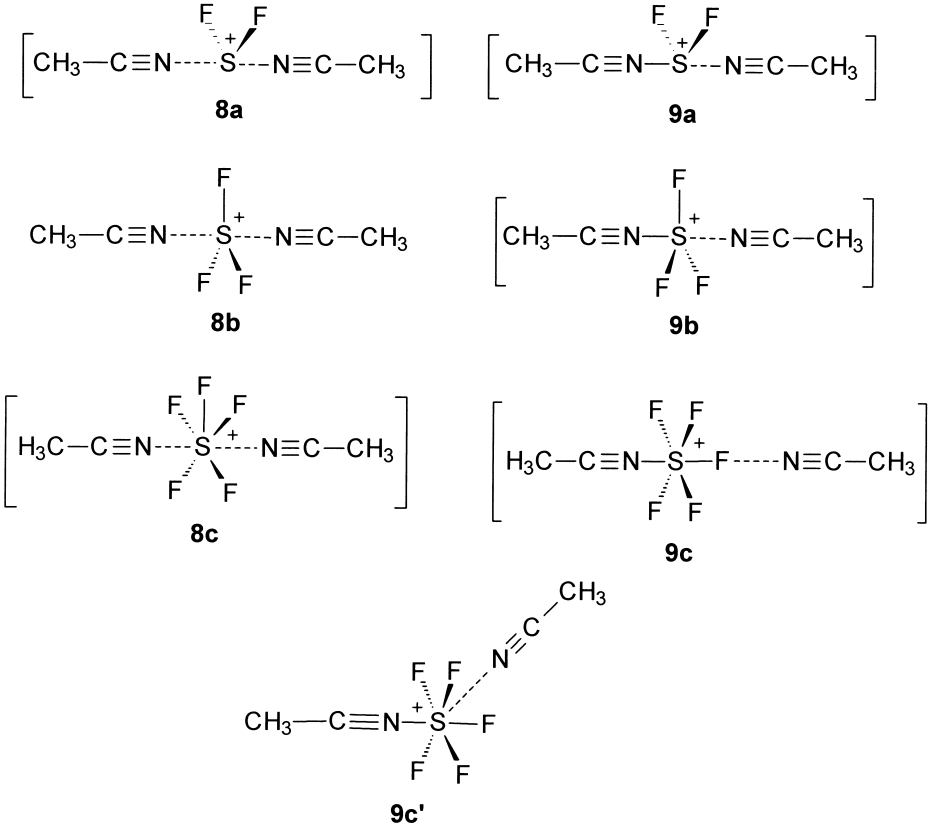

8a **9a** **8b** **9b** **8c** **9c** **9c'**

Scheme 3.

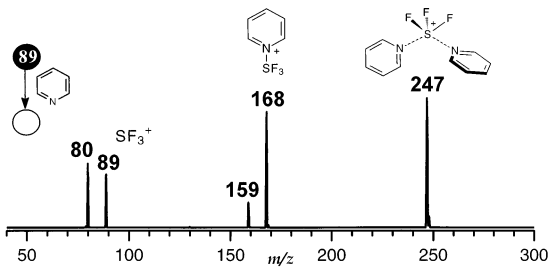

Fig. 3. Double-stage (MS^2) product spectra for reaction of $^{32}SF_3^+$ (*m/z* 89) with pyridine.

Ph–$SF^{+\cdot}$ (**4**) from SF^+ and benzene is overall exothermic by −13.3 kcal/mol. This thermochemistry for SF^+/benzene reactions agrees well with the experimental results [Fig. 1(a)] as no stable $BzSF^+$ adduct is formed but H-by-$SF^{+\cdot}$ replacement occurs to a considerable extent.

Of the three structures considered for the $BzSF_3^+$ adduct, two are stable: **1b** ($n = 3$) and **3b** ($n = 3$). The 1,4-dicoordinated adduct **2b** converges spontaneously to **1b**. The loosely bonded π-adduct **3b** (Fig. 4) is far the most stable $BzSF_3^+$ adduct, −19.1 kcal/mol more stable than the Wheland-type adduct **1b** (Table 2). The potential energy surface for SF_3^+/benzene reactions [Fig. 5(b)] shows a −10.5 kcal/mol enthalpy of formation for **1b**, and −29.5 kcal/mol for **3b**. Contrary to the overall exothermic formation of Ph–$SF^{+\cdot}$ via **1a** [Fig. 5(a)], formation of the analogous Ph–$SF_3^{+\cdot}$ via H loss from the most favorable **3b** adduct is highly endothermic, a process that should be further hampered by a higher energy barrier. HF loss from **3b** to Ph–SF_2^+ is, however, thermodynamically favorable [Fig. 5(b)], but no HF loss was observed for the $BzSF_3^+$ adduct [Fig. 1(b)]. π Coordination in **3b** [Fig. 5(b)] leads to substantial separation between the F and H atoms; hence, HF loss is likely hampered by a high energy barrier.

The finding that the π-coordinated ion **3b** is the most stable $BzSF_3^+$ adduct suggested that it could be possible to form an interesting symmetrically bonded "sandwich"-type $Bz_2SF_3^+$ dimer, **18** (Scheme 5). The

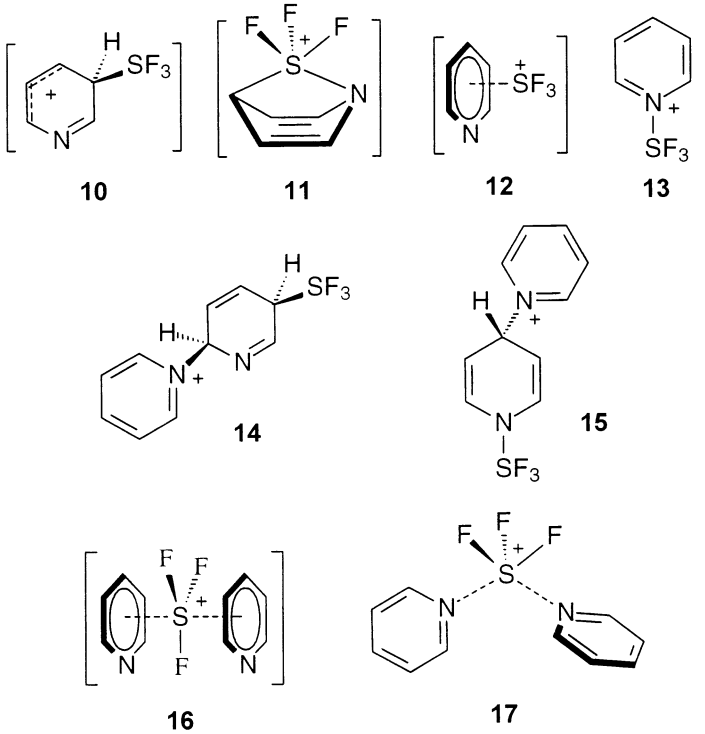

Scheme 4.

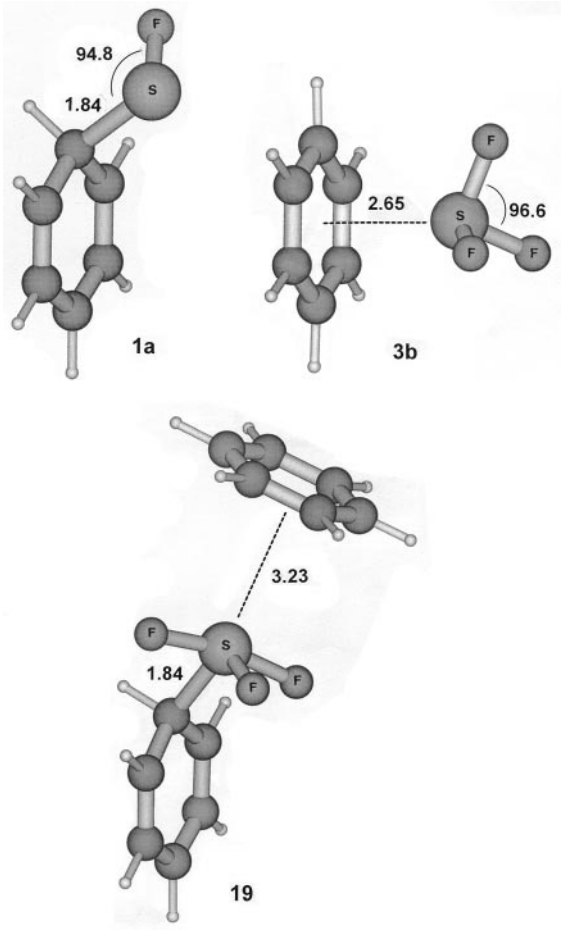

Fig. 4. Ab initio optimized structures for the most stable SF_n^+ adducts and dimers with benzene.

ab initio calculations show, however, that **18** is unstable; it collapses during geometry optimization to a peculiar and unsymmetrically bonded structure, **19** (Fig. 4). In **19**, SF_3^+ is covalently bonded to a benzene molecule and loosely bonded, π coordinated to the other. Although **19** is stable according to the calculations, its formation from **3b** is thermodynamically unfavorable, i.e. endothermic by +10.0 kcal/mol (Table 3).

Reactions of SF_3^+ with benzene [Fig. 1(b)] that fail to form $Bz_2SF_3^+$ also suggest that formation of the $Bz_2SF_3^+$ dimer from the $BzSF_3^+$ adduct is unfavorable. A range of higher benzene pressures in q2 and different collisions energies near 1 eV were also used in unsuccessful attempts to form $Bz_2SF_3^+$.

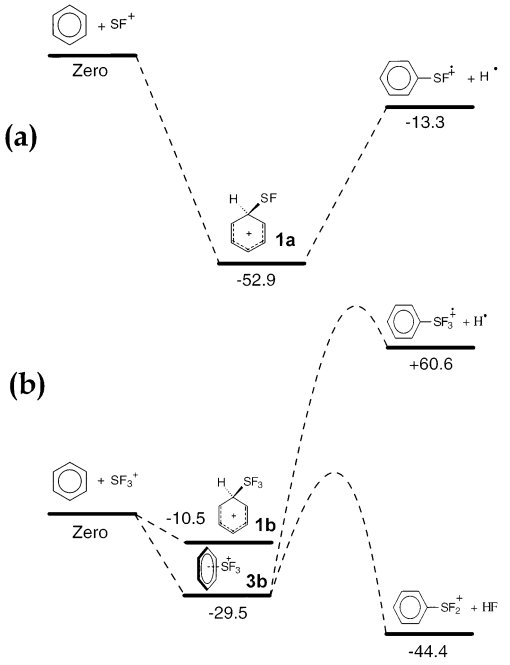

Fig. 5. Ab initio partial potential energy surface diagrams for reactions with benzene of (a) SF^+ and (b) SF_3^+.

3.2.2. Acetonitrile

Fig. 6 compares the optimized structures of the observed acetonitrile adducts: $CH_3CN/SF_2^{+\cdot}$ (**5**), CH_3CN/SF_3^+ (**6**), and CH_3CN/SF_5^+ (**7**). Short N–S bond lengths characterize **5** (1.56 Å) and **7** (1.79 Å) as covalently bonded. Adduct **6** displays, however, a loosely bonded structure with a much longer N–S bond (2.48 Å); **6** is therefore stabilized mainly by electrostatic forces. Note also the characteristic distonic [29] electronic distribution of $CH_3CN–SF_2^{+\cdot}$ (**5**); the positive charge is mainly on the sulfur atom whereas the cyano carbon bears most of the odd spin density.

Ab initio calculations (Table 3) predict positive BDEs, i.e. exothermic enthalpies of formation for both **6** and **7**, whereas the distonic **5** is formed in a slightly endothermic reaction (+8.0 kcal/mol). The increasing $CH_3CN–SF_n^+$ bond energies: $CH_3CN–SF_2^{+\cdot} < CH_3CN\cdots SF_3^+ < CH_3CN–SF_5^+$ (Table 3) probably result in part from the increasing electron deficiency on the coordinating sulfur atom. From MP2/

Table 2
Total, zero point vibrational and relative energies from ab initio calculations

Species[a]	MP2/6-31G(*d*,*p*)//HF/6-31G(*d*,*p*) (hartree)	ZPE[b] (hartree)	MP2/6-31G(*d*,*p*)//HF/6-31G(*d*,*p*) + ZPE (hartree)
Benzene	−231.504 58	0.095 51	−231.409 07
Acetonitrile	−132.357 16	0.043 26	−132.313 90
Pyridine	−247.520 03	0.084 66	−247.435 38
HF	−100.194 12	0.009 11	−100.185 01
H	−0.498 23	Zero	−0.498 23
SF^+	−496.811 17	0.002 23	−496.808 94
$SF_2^{+\cdot}$	−596.428 21	0.005 27	−596.422 95
SF_3^+	−696.059 03	0.009 38	−696.049 65
SF_5^+	−895.187 51	0.017 64	−895.169 87
1a	−728.401 85	0.099 52	−728.302 33
1b	−927.581 70	0.106 27	−927.475 44
3b	−927.612 04	0.106 19	−927.505 85
4	−727.828 80	0.087 85	−727.740 95
5	−728.774 56	0.050 46	−728.724 10
6	−828.466 69	0.053 96	−828.412 73
7	−1027.623 80	0.063 56	−1027.560 24
8b	−960.862 01	0.098 26	−960.763 75
9a	−861.164 82	0.094 81	−861.070 01
9c	−1159.996 42	0.107 35	−1159.889 07
13	−943.656 13	0.097 21	−943.558 92
14	−1191.209 08	0.185 54	−1191.023 54
15	−1191.203 47	0.185 67	−1191.017 80
17	−1191.226 04	0.182 29	−1191.043 75
19	−1159.101 51	0.20244	−1158.899 07
$Ph–SF_2^+$	−827.437 49	0.093 10	−827.344 39
$Ph–SF_3^{+\cdot}$	−926.958 85	0.095 01	−926.863 84

[a] Several adducts and dimers are unstable according to the calculations, see the text.
[b] ZPE energies were scaled by 0.89.

6-31G(*d*,*p*)//HF/6-31G(*d*,*p*) calculations, the Mülliken charges on sulfur are: $SF_2^{+\cdot}$ (+1.55), SF_3^+ (+1.78), and SF_5^+ (+2.14).

Fig. 7 compares the optimized structures of the acetonitrile dimers: $(CH_3CN)_2SF_2^{+\cdot}$ (**9a**), $(CH_3CN)_2SF_3^+$ (**8b**), and $(CH_3CN)_2SF_5^+$ (**9c**). Only **8b** is symmetrically (and loosely) bonded; this finding suggests that SF_3^+

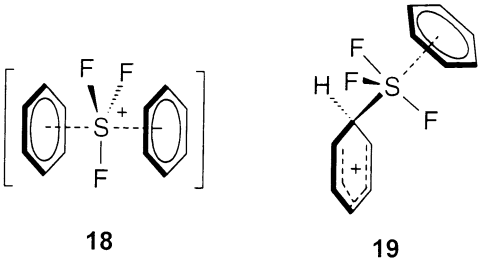

Scheme 5

Table 3
Bond dissociation energies of most stable SF_n^+ adducts and dimers calculated at the MP2/6-31G(*d*,*p*)//6-31G(*d*,*p*) + ZPE level

Species	Products	BDE (kcal/mol)
1a	$C_6H_6 + SF^+$	52.9
3b	$C_6H_6 + SF_3^+$	29.6
5	$CH_3CN + SF_2^{+\cdot}$	−8.0
6	$CH_3CN + SF_3^+$	30.9
7	$CH_3CN + SF_5^+$	48.0
8b	$CH_3CN \cdots SF_3^+ + CH_3CN$	23.4
	$2CH_3CN + SF_3^+$	54.2
9a	$CH_3CN\text{-}SF_2^{+\cdot} + CH_3CN$	20.1
	$2CH_3CN + SF_2^{+\cdot}$	12.1
9c	$CH_3CN–SF_5^+ + CH_3CN$	9.4
	$2CH_3CN + SF_5^+$	57.4
13	$C_5H_5N + SF_3^+$	46.4
17	$C_5H_5N—SF_3^+ + C_5H_5N$	30.9
	$2C_5H_6N + SF_3^+$	77.4
19	$C_6H_6 \cdots SF_3^+ + C_6H_6$	−10.0
	$2C_6H_6 + SF_3^+$	19.7

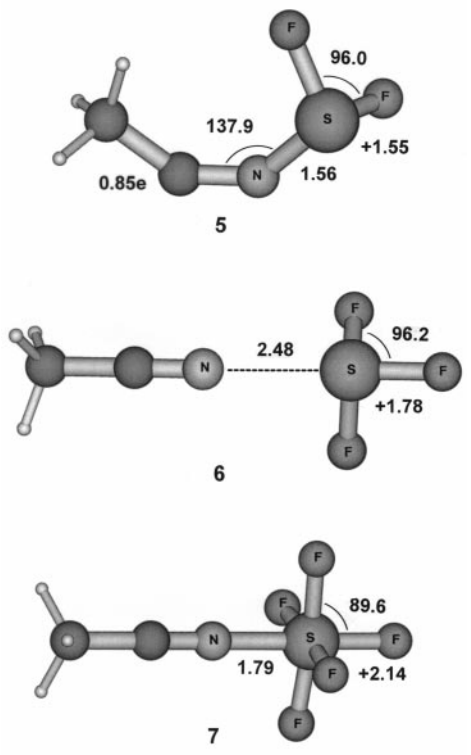

Fig. 6. Ab initio optimized structures for the most stable SF_n^+ adducts with acetonitrile.

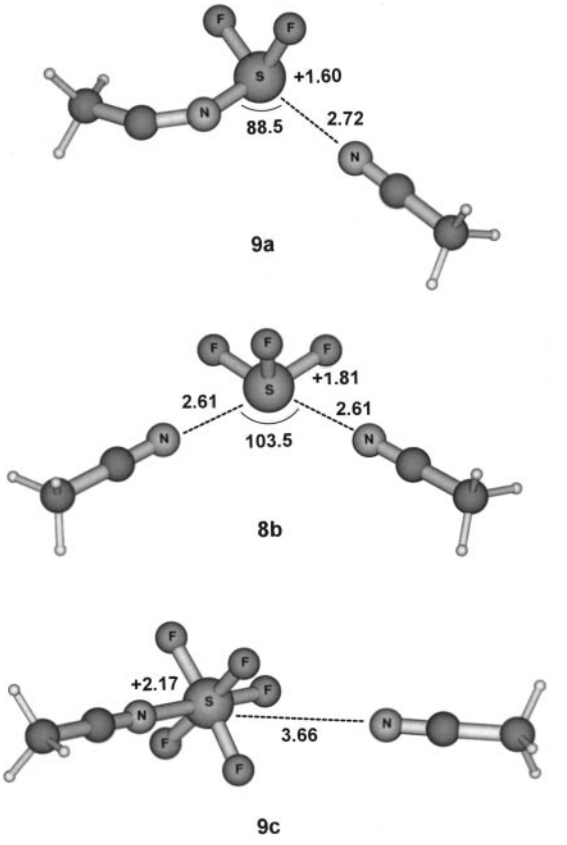

Fig. 7. Ab initio optimized structures for the most stable SF_n^+ dimers with acetonitrile.

nitrile affinities should be appropriately estimated by measuring dissociation proclivities of mixed $[R^1CN \cdots SF_3 \cdots NCR^2]^+$ dimers. But for the unsymmetrically bonded structures **9a** and **9c′** to provide reliable $SF_2^{+\cdot}$ and SF_5^+ nitriles affinities via the Cooks' kinetic method [19], the two isomeric forms $[R^1CN–SF_n \cdots NCR^2]^+$ and $[R^1CN \cdots SF_n–NCR^2]^+$ must rapidly interconvert.

3.2.3. Pyridine

Of the four $PySF_3^+$ adducts (**10–13**), only the covalently bonded N-coordinated **13** is stable (Table 2). Of the four $Py_2SF_3^+$ dimers, three are stable: **14**, **15**, and **17** (Table 2); the fourth, sandwich-type dimer **16** is unstable and collapses to **17** during geometry optimization. The N-coordinated, loosely but unsymmetrically bonded **17** is far the most stable dimer (Table 2), with a BDE (to SF_3^+) as high as 77.4 kcal/mol (Table 3). Because the analogous $Bz_2SF_3^+$ sandwich-type dimer **18** was found to spontaneously isomerize to **19** (Scheme 5), a similar species, **20** (Scheme 6), was also considered for the $Py_2SF_3^+$ dimer. However, **20** is found unstable; it isomerizes spontaneously to **17** during geometry optimization.

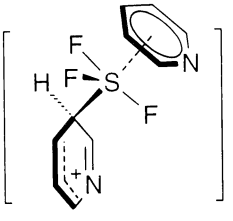

20

Scheme 6.

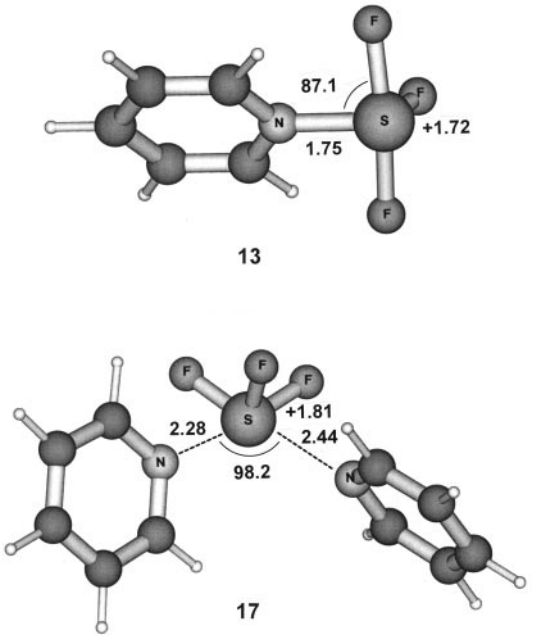

Fig. 8. Ab initio optimized structures for the most stable SF_3^+ adduct and dimer with pyridine.

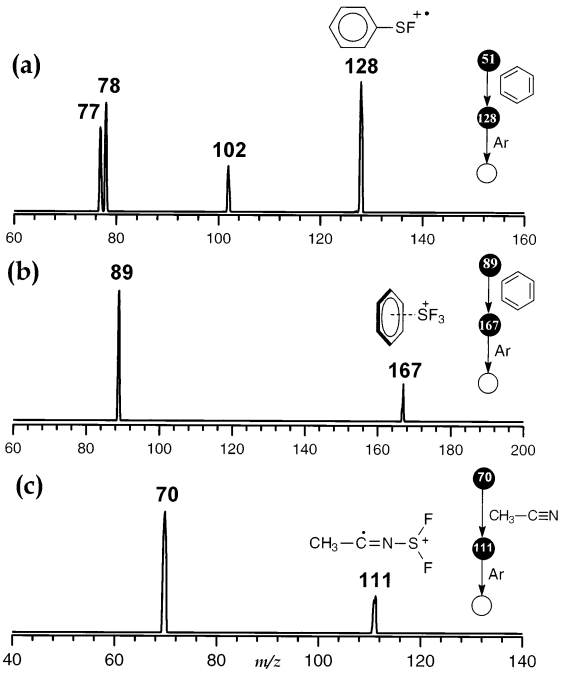

Fig. 9. Triple-stage (MS^3) sequential product spectra of (a) C_6H_5–$SF^{+\cdot}$; (b) the $BzSF_3^+$ adduct, and (c) the $CH_3CN/SF_2^{+\cdot}$ adduct.

Fig. 8 compares the optimized structure of the most stable, most thermodynamically favorable $PySF_3^+$ adduct (**13**) and $Py_2SF_3^+$ dimer (**17**). Adduct **13** is covalently bonded, with a trigonal bipyramid geometry in which both the pyridine ring and the sulfur lone pair of electrons occupy equatorial positions. The optimized structure of **17** clearly characterize a loosely and unsymmetrically bonded species in which steric hindrance forces the two pyridine rings to assume an orthogonal alignment that results in different N–S bond lengths; 2.28 and 2.44 Å. Low energy isomerism is expected, however, to rapidly interconvert the two N–S bonds, as indicated by the linear correlation between proton and SF_3^+ affinities of unhindered pyridines obtained via the application of the Cooks' kinetic method [18].

3.2.4. Triple stage mass spectra

Structural information of reaction products was accessed by recording triple-stage (MS^3) sequential product spectra [23]. The product of *m/z* 128 [Fig. 9(a)] formed in SF^+ reactions with benzene dissociates likely by loss of C_2H_2 (*m/z* 102), C_4H_2 (*m/z* 78), and $SF^{\cdot}$ (*m/z* 77). Such dissociation behavior agrees wll with the expected structure of the ion, i.e. C_6H_5–$SF^{+\cdot}$ (**4**). The triple-stage spectrum displayed in Fig. 9(a) is probably the first MS data collected for benzenesulfenyl fluoride.

The $BzSF_3^+$ [Fig. 9(b)] and CH_3–CN/SF_5^+ adducts, and the $(CH_3–CN)_2SF_5^+$, $(CH_3–CN)_2SF_2^{+\cdot}$ [Fig. 9(c)] and $Py_2SF_5^+$ dimers, dissociate exclusively and extensively to reform the corresponding SF_n^+ ion, easy cleavages that suggest loosely bonded structures [19] such as those predicted by the ab initio calculations. The distonic CH_3–CN–$SF_2^{+\cdot}$ (**5**) is predicted to be covalently bonded by the calculations, but to display an exothermic dissociation threshold to SF_2^+ (Table 3). Therefore, the extensive dissociation of **5** to SF_2^+ of *m/z* 70 under collision activation [Fig. 9(c)] also agrees with the theoretical prediction.

4. Conclusion

From both a systematic investigation on the gas-phase intrinsic coordination ability of SF_n^+ ions (n = 1–5) with benzene, acetonitrile, and pyridine, and from formation enthalpies, bond dissociation energies, and most likely structures of adducts and dimers predicted by ab initio calculations, the following reactivity trends are derived; $SF_4^{+\cdot}$ does not coordinate with any of the π-electron rich neutrals employed—benzene, acetonitrile, and pyridine; instead $SF_4^{+\cdot}$ loses F or reacts by charge transfer, or both. SF_3^+ displays by far the greatest coordination ability; it forms both adducts and dimers with acetonitrile and pyridine, and an adduct with benzene, which are all loosely bonded. With acetonitrile only, $SF_2^{+\cdot}$ and SF_5^+ form covalently bonded adducts and unsymmetrically bonded dimers. SF^+ coordinates only with benzene, but the nascent $BzSF^+$ adduct is formed with excess of internal energy; hence, it rapidly loses H to form ionized benzenesulfenyl fluoride, C_6H_5–$SF^{+\cdot}$. Therefore, net H-by-$SF^{+\cdot}$ replacement occurs—a novel benzene reaction.

These findings expand the knowledge of SF_n^+ coordination abilities, serving as a guide to better understand their behavior in chemical processes. Further gas-phase studies can also benefit from the present results, as for instance, measurements of SF_n^+ affinities via the Cooks' kinetic method.

Acknowledgements

This work was supported by the Research Support Foundation of the State of São Paulo (FAPESP) and the Brazilian National Research Council (CNPq).

References

[1] I. Sauers, H.W. Ellis, L.G. Christophorou, IEEE Trans. Electr. Insul. EI-21 (1986) 111.
[2] J.W. Cob, Plasma Chem. Plasma Process 2 (1982) 1.
[3] J.A. Stone, W.J. Wytenberg, Int. J. Mass Spectrom. Ion Processes 94 (1989) 269.
[4] (a) L.M. Babcock, G.E. Streit, J. Chem. Phys. 75 (1981) 3868; (b) J.L. Lyman, R.J. Jensen, J. Phys. Chem. 77 (1973) 883; (c) C.L. Chen, P.J. Chantry, J. Chem. Phys. 71 (1979) 2897.
[5] (a) E.R. Grant, M.J. Coggiola, Y.T. Lee, P.A. Schulz, Aa.S. Subdo, Y.R. Shen, Chem. Phys. Lett. 52 (1977) 595; (b) L. Lyman, J. Chem. Phys. 67 (1977) 1868.
[6] R.D. McAlpine, D.K. Evans, Adv. Chem. Phys. 60 (1985) 31.
[7] K.A. Mitchell, Chem. Rev. 69 (1969) 157.
[8] (a) G.C. Demitras, A.G. MacDiarmid, Inorg. Chem. 3 (1964) 1198; (b) H.L. Roberts, Q. Rev.(London) 15 (1961) 30; (c) J.R. Case, F. Nyman, Nature 193 (1962) 473.
[9] (a) L.M. Babcock, G.E. Streit, J. Chem. Phys. 75 (1981) 3864; (b) F.C. Fehsenfeld, ibid. 54 (1971) 438.
[10] C.Q. Jiao, B.S. Freiser, J. Am. Chem. Soc. 115 (1993) 6268.
[11] (a) Y.-S. Cheung, Y.-J. Chen, C.Y. Ng, S.-W. Chiu, W.-K. Li, J. Am. Chem. Soc. 117 (1995) 9725; (b) K.K. Irikura, J. Chem. Phys. 102 (1995) 5357, and references therein.
[12] (a) H.-X. Wang, J.H. Moore, J.K. Olthoff, R.J. van Brunt, Plasma Chem. Plasma Process 13 (1993) 1; (b) R.J. van Brunt, J.T. Herron, IEEE Trans. Electrical Insulation 25 (1990) 76.
[13] A. Tamura, K. Inoue, T. Onuma, M. Sato, Appl. Phys. Lett 51 (1987) 1503.
[14] K. Hiraoka, A. Shimizu, A. Minamitsu, M. Nasu, S. Fujimaki, S. Yamabe, J. Am. Soc. Mass Spectrom 6 (1995) 1137.
[15] J.G. Dillard, J.H. Troester, J. Phys. Chem. 23 (1975) 2455.
[16] (a) R. Zangerie, A. Hansel, R. Richter, W. Lindinger, Int. J. Mass Spectrom. Ion Processes 123 (1993) 117; (b) R. Richter, P. Tosi, W. Lindinger, J. Chem. Phys. 87 (1993) 4615.
[17] A.Z. Karachevtev, A.Z. Maratkin, V.V. Savkin, V.L. Tal'rose, Sov. J. Chem. Phys. 3 (1985) 695.
[18] P.S.H. Wong, S. Ma, S.S. Yang, R.G. Cooks, F.C. Gozzo, M.N. Eberlin, J. Am. Soc. Mass Spectrom 8 (1996) 68.
[19] (a) R.G. Cooks, J.S. Patrick, T. Kotiaho, S.A. McLuckey, Mass Spectrom. Rev. 13 (1994) 287; (b) M.N. Eberlin, T. Kotiaho, B.J. Shay, S.S. Yang, R.G. Cooks, J. Am. Chem. Soc. 116 (1994) 2457; (c) P.S.H. Wong, S. Ma, S.S. Yang, R.G. Cooks, F.C. Gozzo, M.N. Eberlin, J. Am. Soc. Mass Spectrom. 8 (1997) 68.
[20] R. Sparrapan, M.A. Mendes, I.P.P. Ferreira, M.N. Eberlin, C. Santos, J.C. Nogueira, J. Phys. Chem. A 102 (1998) 5189.
[21] For a review see: M.N. Eberlin, Mass Spectrom. Rev. 16 (1997) 113.
[22] V.F. Juliano, F.C. Gozzo, M.N. Eberlin, C. Kascheres, C.L. Lago, Anal. Chem. 68 (1996) 1328.
[23] J.C. Schwartz, A.P. Wade, C.G. Enke, R.G. Cooks, Anal. Chem. 62 (1990) 1809.
[24] (a) M.N. Eberlin, A.E.P.M. Sorrilha, F.C. Gozzo, R. Sparrapan, J. Am. Chem. Soc. 119 (1997) 3550; (b) L.A.B. Moraes, F.C. Gozzo, M.N. Eberlin, P. Vainiotalo, J. Org. Chem. 62 (1997) 5096; (c) M. Carvalho, R. Sparrapam, M.A. Mendes, C. Kascheres, M.N. Eberlin, Chem. Eur. J. 4 (1998) 1161; (d) M.A. Mendes, L.A.B. Moraes, R. Sparrapan, M.N. Eberlin, R. Kostiainen, T. Kotiaho J. Am. Chem. Soc. 120 (1998) 7869; (e) L.A.B.M. Moraes, M.N. Eberlin, ibid. 120 (1998) 11136.
[25] T.O. Tiernan, J.H. Futrell, J. Phys. Chem. 72 (1968) 3080.
[26] GAUSSIAN94, Revision B.3, M.J. Frisch, G.W. Trucks, H.B. Schlegel, P.M.W. Gill, B.G. Johnson, M.A. Robb, J.R.

Cheeseman, T. Keith, G.A. Petersson, J.A. Montgomery, K. Raghavachari, M.A. Al-Laham, V.G. Zakrzewski, J.V. Ortiz, J.B. Foresman, C.Y. Peng, P.Y. Ayala, W. Chen, M.W. Wong, J.L. Andres, E.S. Replogle, R. Gomperts, R.L. Martin, D.J. Fox, J.S. Binkley, D.J. Defrees, J. Baker, J.P. Stewart, M. Head-Gordon, C. Gonzalez, J.A. Pople, Gaussian, Inc., Pittsburgh PA, 1995.

[27] L.A. Curtis, K. Raghavachari, J.A. Pople, J. Chem. Phys. 98 (1993) 1293.

[28] C. Møller, M.S. Plesset, Phys. Rev. 46 (1934) 618.

[29] (a) S. Hammerum, Mass Spectrom. Rev. 7 (1988) 123; (b) G. Bouchoux, Mass Spectrom Rev. 7 (1988) 203; (c) K.M. Stirk, M.L.K. Kiminkinen, H.I. Kenttämaa, Chem. Rev. 92 (1992) 1649.